VERSITA

CELLULAR & MOLECULAR BIOLOGY LETTERS
http://www.cmbl.org.pl

Received: 23 July 2009
Final form accepted: 08 October 2009
Published online: 15 October 2009

Volume 15 (2010) pp 55-69
DOI: 10.2478/s11658-009-0034-0

Research article

ESTABLISHING AND FUNCTIONAL CHARACTERIZATION OF AN HEK-293 CELL LINE EXPRESSING AUTOFLUORESCENTLY TAGGED β-ACTIN (pEYFP-ACTIN) AND THE NEUROKININ TYPE 1 RECEPTOR (NK1-R)

ALENKA HROVAT[1], APOLONIJA BEDINA ZAVEC[2], AZRA POGAČNIK[1], ROBERT FRANGEŽ[3] and MILKA VRECL[1]*

[1]Institute of Anatomy, Histology and Embryology, Veterinary Faculty, Gerbičeva 60, SI-1000 Ljubljana, Slovenia, [2]Institute of Chemistry, Hajdrihova 19, SI-1000 Ljubljana, Slovenia, [3]Institute of Physiology, Pharmacology and Toxicology, Veterinary Faculty, Gerbičeva 60, SI-1000 Ljubljana, Slovenia

Abstract: This study focused on establishing and making a comprehensive functional characterization of an HEK-293-transfected cell line that would coexpress the enhanced yellow fluorescent protein-actin (pEYFP-actin) construct and the neurokinin type 1 receptor (NK1-R), which is a member of the seven transmembrane (7TM) receptor family. In the initial selection procedure, the cloning ring technique was used alone, but failed to yield clones with homogenous pEYFP-actin expression. Flow cytometry sorting (FCS) was

* Author for correspondence. E- mail: milka.vrecl@vf.uni-lj.si

Abbreviations used: 7TM – seven transmembrane receptor; B_{max} – max. receptor number; BSA – bovine serum albumin; Ct – threshold cycle; DMEM – Dulbecco's modified Eagles's Medium; DNA – deoxyribonucleic acid; D-PBS – Dulbecco's phosphate-buffered saline; ELISA – enzyme-linked immunosorbent assay; F-actin – filamentous actin; FCA – flow cytometry analysis; FCS – flow cytometry sorting; GFP – green fluorescent protein; GPCR – G-protein coupled receptor; HA – hemagglutinin; HANK1-R – N-terminally HA-tagged human neurokinin-1 receptor; HEK-293 – human embryonic kidney cells; HIFCS – heat inactivated fetal calf serum; HRP – horseradish peroxidase; IC_{50} – 50% inhibitory concentration; IP1 – inositol phosphate 1; mRNA – messenger ribonucleic acid; NK1-R – neurokinin type 1 receptor; pEYFP – enhanced yellow fluorescent protein; PN – passage number; RT – reverse transcription; RT-PCR – quantitative real-time reverse transcription / polymerase chain reaction; SP – substance P; TMB – tetramethylbenzidine; WT – wild-type

subsequently used to enrich the pEYFP-actin-expressing subpopulation of cells. The enzyme-linked immunosorbent assay (ELISA), FCS and quantitative real-time reverse transcription/polymerase chain reaction (RT-PCR) were then employed to monitor the passage-dependent effects on transgene expression and to estimate the total β-actin/pEYFP-actin ratio. NK1-R was characterized via radioactive ligand binding and the second messenger assay. The suitability of the pEYFP-actin as a marker of endogenous actin was assessed by colocalizing pEYFP-actin with rhodamine-phalloidine-stained F-actin and by comparing receptor- and jasplakinolide-induced changes in the actin cytoskeleton organization. These experiments demonstrated that: i) both constructs expressed in the generated transfected cell line are functional; ii) the estimated pEYFP-actin:endogenous β-actin ratio is within the limits required for the functional integrity of the actin filaments; and iii) pEYFP-actin and rhodamine-phalloidine-stained F-actin structures colocalize and display comparable reorganization patterns in pharmacologically challenged cells.

Key words: Cytoskeleton, Actin filaments, HEK-293, Neurokinin type 1 receptor, Flow cytometry, Confocal microscopy

INTRODUCTION

The reorganization of the actin cytoskeleton is an important cellular response to extracellular signals. This is a process that can also be mediated by several seven transmembrane receptors (7TM receptors; also called G-protein coupled receptors, GPCRs) and their cognate heterotrimeric G-proteins [1-3]. However, this cytoskeletal reorganization cannot easily be studied using images of fixed cells. That presented researchers with several difficulties in understanding its spatial and temporal organization [4, 5]. The development of green fluorescent protein-based (GFP-based) technology greatly contributed to the visualization, tracking and quantification of proteins within living cells. GFP from the jellyfish *Aequorea victoria* and its variants can be fused to basically any protein of interest (reviewed in [6]). This approach has also been successfully applied to cytoskeleton imaging in live cells [4, 5, 7], 7TM receptor research (e.g. gene expression, subcellular localization and trafficking studies) [8] and the drug discovery process [9]. However, the GFP-based approach has seldom been used to study the role of 7TM receptors in the regulation of actin reorganization and *vice versa*. There have only been a few recent studies that employed 7TM receptor-GFP fusion constructs and rhodamine-phalloidine staining of actin, and revealed a possible regulatory role of the actin cytoskeleton in receptor internalization [10] and signaling [11]. Studies focusing on the involvement of various G_α protein subunits in the 7TM receptor-mediated actin cytoskeleton rearrangement were mostly performed with transiently transfected cells or cells microinjected with the protein of interest [12-15]. The disadvantages of these methods are the short experimental time due to proteolysis or the transient

expression of the proteins of interest, the differences in the expression levels of the proteins among the trasfected cells, and the potential for mechanical injury to the cells when using microinjection [16, 17]. Having a transfected cell line that expresses the 7TM receptor of interest, i.e. $G_{\alpha q/11}$-coupled neurokinin type 1 receptor (NK1-R) and β-actin tagged with enhanced yellow fluorescent protein (pEYFP) therefore facilitates the performance of various fluorescence imaging work, and presents a stable source of proteins that could be critical for the reproducibility of results [16, 17].

However, the following difficulties can be encountered when generating a stable cell line: i) the clonal cell lines obtained via ring-cloning may be heterogenous, often due to the contamination of the clonal cells with the surrounding cells [18]; ii) there may be an unsatisfactory expression level of the transgene, since the percentage of cells expressing the protein of interest is usually high, but the level of the expressed protein is low; and iii) there is the possibility of interference from fusion proteins with the normal structure and function of the endogenous proteins [6, 17]. The aim of this study was to generate and functionally characterize a transfected cell line expressing both NK1-R and pEYFP-actin, as having such a cell line would enable visualization of the receptor-mediated alterations of actin cytoskeletal structures in live cells.

MATERIAL AND METHODS

Materials

The molecular biology reagents were obtained either from Invitrogen (Carlsbad, CA, USA) or Qiagen (Crawley, West Sussex, UK). All the tissue media and reagents were purchased either from Gibco Invitrogen (Carlsbad, CA, USA) or Sigma Aldrich (St. Louis, MO, USA) unless otherwise stated. The anti-hemagglutinin (HA) high-affinity rat monoclonal antibodies were from Roche (Basel, Switzerland), and the anti-rat horseradish peroxidase-conjugated (HRP-conjugated) antibodies were from Sigma Aldrich (St. Louis, MO, USA).

Expression constructs

N-terminally HA-tagged human neurokinin-1 receptor (HANK1-R) in the vector pcDNA3.1 was made using standard molecular biology techniques and was verified by sequencing. The construct was as previously characterized [19, 20]. EYFP-tagged β-actin (pEYFP-actin) was purchased from BD Biosciences (Clontech, San Jose, CA, USA). The EYFP variant of the *Aequorea victoria* GFP has its excitation and fluorescence emission peaks respectively at 513 and 527 nm.

Cell culture and transfection

HEK-293 cells (European Collection of Animal Cell Cultures, Salisbury, UK) were routinely maintained and passaged in Dulbecco's modified Eagle's Medium (DMEM) supplemented with 10% (v/v) heat-inactivated fetal calf serum (HIFCS), 2 mM Glutamax^{TM}-I, penicillin (100 U/ml) and streptomycin

(100 μg/ml), and incubated at 37ºC in a humidified atmosphere of 5% (v/v) CO_2 in air. The cells were co-transfected with HANK1-R and pEYFP-actin using Lipofectamine™. Receptor- and pEYFP-actin-expressing clones were selected by geneticin (1 mg/ml), and individual clones were isolated via the cloning ring technique as previously described by McFarland [18].

Flow cytometry analyses and sorting

Flow cytometric analyses (FCA) and cell sorting (FCS) were performed with an EPICS Altra cell sorter (Beckman Coulter Electronics, Fullerton, CA, USA) equipped with a 488-nm water-cooled laser. For the FCA of the pEYFP-actin expression, the cells were washed once in Dulbecco's phosphate-buffered saline (D-PBS) and resuspended in D-PBS containing 3% bovine serum albumin (BSA; Sigma, St Louis, MO, USA) at a density of 10^6 cells/ml. After the excitation of pEYFP-actin with 488-nm laser light, the emitted fluorescence was collected through a 520-530 nm band pass filter. A minimum of 10,000 cells were used for the analysis and subjected to flow cytometry sorting. The cell subpopulation exhibiting high green fluorescence intensity was selected for sorting. Flow-sorted cells were grown in complete medium with geneticin (1 mg/ml), and then functionally characterized. The data analysis and graphics were acquired using EXPO32 software.

Receptor-binding assay

A self-competition radioligand-binding assay was carried out on a transfected cell line expressing NK1-R and pEYFP-actin (designated HEK-NK1-R+pEYFP-actin) in 24-well plates. The cells were incubated with [^{125}I]-Substance P ([^{125}I]-SP; Bolton Hunter labelled Lys^3 Substance P; Perkin Elmer; Billerica, MA, USA) in the presence of increasing concentrations of unlabeled SP (at a final concentration of 10^{-12} to 10^{-6} M) in 0.5 ml of assay medium for 3 h at 4ºC. Using a solubilization solution, samples were collected into tubes and the γ radioactivity was counted on a 1275 Minigamma Counter (LKB Wallac, Turku, Finland). The determinations were performed in triplicate. The binding parameters were determined from displacement curves generated via sigmoidal dose-response-curve fitting (GraphPad Prism). The receptor density (B_{max}) was then expressed in femtomoles per 100,000 cells, as previously described [21].

Inositol phosphate 1 (IP1) assay

The IP-One ELISA assay (Cisbio Bioassays, Bagnols-sur-Cèze Cedex, France) was used to determine agonist-induced IP1 generation, which tightly correlates with the $G_{\alpha q/11}$-coupled receptor activity. The HEK-NK1-R+pEYFP-actin-transfected cell line was plated in 24-well plates coated with poly-L-lysine at a density of 1×10^5 cells per well, and incubated overnight. On the day of the experiment, the complete DMEM was removed, and the cells were incubated for 1 h in a stimulation buffer containing 10 mM LiCl and then stimulated with SP (1 μM, 10 min at 37ºC). After stimulation, the cells were lysed and the supernatant transferred into the supplied ELISA plate. The produced IP1 was

detected by adding the ELISA reagents according to the manufacturer's instructions. The absorbance was measured in a Rosys Anthos 2010 microplate reader (Anthos Labtec Instruments, Wals, Austria) at 450 nm. The determinations were made in duplicate. Since this assay is based on the competition between free IP1 and IP1-HRP conjugate for a limited number of binding sites on an anti-IP1 monoclonal antibody, agonist-induced IP1 production is read as a signal reduction. The obtained data, calculated as the percentage of initial signal reduction, was analyzed, and a graph was created using GraphPad Prism computer software (La Jolla, CA, USA).

ELISA of surface-expressed NK1-R

The enzyme-linked immunosorbent assay (ELISA) was performed as described previously [20, 22] to determine the level of surface-expressed HA-tagged NK1-R. Briefly, HEK-NK1-R+pEYFP-actin transfected cells from passage numbers 3, 9 and 15 were seeded out at a density of 1×10^5 cells per well in 24-well plate. After 24 h, the cells were washed three times, fixed, and incubated in blocking solution (5% BSA in PBS) for 30 min at room temperature. The cells were kept at room temperature for all the subsequent steps. First, the cells were incubated for 2 h with rat anti-HA antibodies (1:200 dilution), washed three times, incubated for 1 h with anti-rat HRP-conjugated antibodies (1:1000 dilution), and then extensively washed. The immunoreactivity was revealed by the addition of tetramethylbenzidine (TMB) substrate. The reaction was terminated by the addition of 0.5 N sulfuric acid. The absorbance was measured at 450 nm in a Rosys Anthos 2010 microplate reader (Anthos Labtec Instruments, Wals, Austria). The determinations were made in quadruplicate. The obtained data was analyzed to create a graph using GraphPad Prism computer software (La Jolla, CA, USA).

Quantitative real-time reverse transcription/polymerase chain reaction (RT-PCR)

Quantitative RT-PCR analysis was used to assess the mRNA expression levels of the endogenous β-actin and pEYFP-actin. Total RNA was extracted from HEK-293 and HEK-293 HANK1 pEYFP-actin-transfected cells from passage numbers 3, 9 and 15 according to the instructions for the use of the Qiagen SV total RNA Isolation System (Promega, Madison, WI, USA). 10 μg of each RNA sample was reverse transcribed into the cDNA using a High-capacity cDNA Archive Kit (Applied Biosystems, Foster City, CA, USA) in a final reaction volume of 50 μl. TaqMan® Gene Expression Assays (Hs99999903_m1; Applied Biosystems) were used to detect both endogenous β-actin and pEYFP-actin mRNA, and the Assay-by-Design Service was used to design the primers and fluorescent 6-FAM dye-labeled minor-groove-binder probes to detect the pEYFP-actin mRNA alone. The sequences of primer pairs and probes used to detect pEYFP-actin were: 5-GAGCGCACCATCTTCTTCAAG (sense); 5-TGTCGCCCTCGAACTTCAC (anti-sense); and 5-ACGACGGCAACTACA (probe). The eukaryotic ribosomal (r) 18s RNA (ABI PRISM TaqMan® Pre-

developed Assay Reagent Ribosomal RNA control PN 4310893E) was used as an endogenous control. The real-time polymerase chain reaction (PCR) was then performed with TaqMan universal PCR Master Mix (Applied Biosystems) in a final reaction volume of 20 μl in an AbiPrism 7000 Sequence Detection System as previously described [20]. PCR amplification was carried out for 40 cycles. The results were expressed as the threshold cycle (Ct), i.e. the cycle number at which the PCR product crosses the threshold of detection. The relative quantification of the target transcripts (β-actin and pEYFP-actin) normalized to the endogenous control 18s rRNA was determined by the comparative Ct method (ΔCt) according to the manufacturer's protocol (User Bulletin No. 2, Applied Biosystems). The $2^{-\Delta\Delta Ct}$ method was used to analyze the relative changes in gene expression between the tested cell lines. Control experiments without reverse transcription (RT) were performed to show that there had been no contamination with the genomic DNA.

Confocal microscopy

For the confocal microscopy, cells were grown under standard conditions on 0.01% poly-L-lysine-coated coverslides that were individually placed into 60-mm Petri dishes containing 5 ml of complete DMEM. On the day of the experiment, when the cell density was 60-80%, the complete DMEM was removed and the cells were serum-starved for 2 h at 37ºC in Hepes-buffered DMEM (Sigma). The media was then replaced with buffered DMEM (control cells) or buffered DMEM with the addition of NK1-R agonist SP (1 μM) for 10 min at 37ºC or jasplakinolide (100 nM) for 2 h at 37ºC, and then fixed with 4% paraformaldehyde. For the rhodamine-phalloidine staining of the actin cytoskeleton, the cell membrane was permeabilized with 0.01% Triton X-100 in PBS for 20 min at room temperature. To reduce non-specific binding, the cells were incubated in blocking solution (PBS/1% BSA) for 30 min at room temperature before staining with rhodamine-phalloidine (Molecular Probes, Netherlands). Rhodamine-phalloidine was used at a 1:20 dilution to obtain a comparable staining intensity in the jasplakinolide-treated cells, as jasplakinolide competes with phalloidine for the same binding sites on F-actin [23]. The nuclei were counterstained with TO-PRO-3 iodide (Molecular Probes, Netherlands) in blocking solution. The cells were then mounted with an anti-fading ProLong®Gold reagent (Molecular Probes, Netherlands), sealed, and examined under an oil immersion objective (Planapo 40×, N.A. = 1.25) using a Leica multispectral confocal laser microscope (Leica TCS NT, Heidelberg, Germany). The sequential detection of pEYFP-actin, rhodamine-phalloidine-stained actin structures and nuclei was achieved with excitation laser lines, respectively at 488 nm (Argon), 543 nm and 633 nm (Helium-Neon). The fluorescence from the channels was collected sequentially and images produced with an 8-fold frame averaging at a resolution of 1024×1024 pixels. Optical sections (1.0 μm) were taken, and representative sections corresponding to the middles of the cells were prepared using Adobe Photoshop 7.0 computer software.

RESULTS

Transfected cell line generation

Using the classical cloning ring technique, we isolated ten clones and assessed the expression levels of NK1-R via the radioligand-binding assay and those of pEYFP-actin via confocal microscopy. As depicted in Fig. 1, in only four of the isolated clones was the level of surface-expressed NK1-R above the background. Furthermore, the confocal microscopy revealed that only a small subpopulation of the cells in these clones expressed detectable levels of pEYFP-actin (data not shown). We therefore selected the clone that expressed the highest level of NK1-R and subjected it to flow cytometry analysis (FCA) and cell sorting (FCS) to enrich the pEYFP-actin-expressing subpopulation of cells. FCA revealed that only about 0.1% of the HEK-NK1-R+pEYFP-actin cells expressed measurable levels of the pEYFP-tagged actin prior to FCS (data not shown). An initial sorting step was then performed to enrich the cells of interest, followed by a second sorting step using the same gate that resulted in about 60% of cells expressing the pEYFP-actin (designated HEK-NK1-R+pEYFP-actin) that was subsequently subjected to functional characterization.

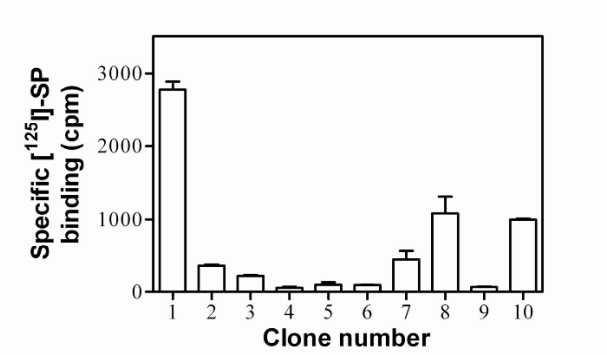

Fig. 1. The plasma membrane expression of the NK1-R receptor in clones obtained via the cloning ring technique. Isolated clones were assessed for NK1-R surface expression by their ability to bind [^{125}I]-SP in a whole-cell binding assay. The total binding was measured in the absence of a competitor, and non-specific binding was determined in the presence of 10^{-6} M unlabeled NK1-R agonist SP. The data is presented as the mean ± S.D. of triplicate observations from a single experiment.

Transfected cell line characteristics – NK1-R expression and signaling properties

A pharmacological characterization of the HEK-NK1-R+pEYFP-actin-transfected cell line was done using radioligand binding assays and IP1 measurements. In self-competition assays, SP competed for binding with ^{125}I-SP with an affinity of 0.88 ± 0.17 nM, and the calculated receptor number (B_{max}) was ~12.1 fmol/100,000 cells (i.e. ~72,860 receptors/cell). The obtained IC_{50} value concurs with those previously published for human WT and HA-tagged NK1-R [20, 24]. The second messenger function of the NK1-R was assessed by IP1 measurements. SP-induced IP1 generation reduced the initial IP1 signal by

around 75%. Once the functionality of the NK1-R in the transfected cell line was established, we utilized ELISA, which is a non-radioactive detection method, to monitor the passage-dependent effect on the NK1-R plasma membrane expression. The ELISA results showed that at all three tested passage numbers (PN3, PN9 and PN15), the plasma membrane expression of NK1-R was comparable (Fig. 2A).

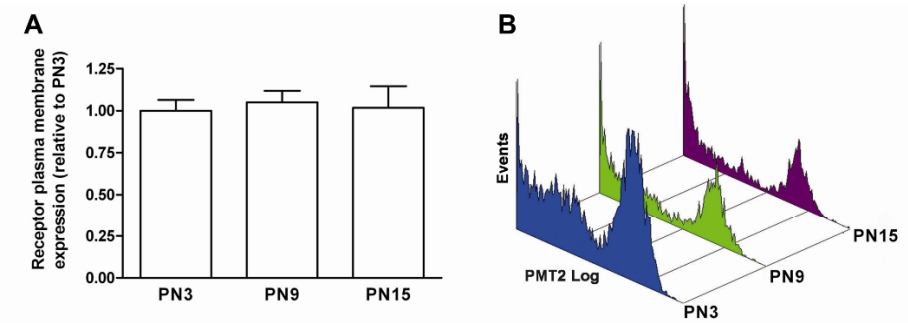

Fig. 2. The influence of passage number on NK1-R and pEYFP-actin expression. A – The plasma membrane expression of NK1-R based on ELISA was determined in passage numbers 3, 9 and 15 of the HEK-NK1-R+pEYFP-actin transfected cell line as described in the Material and Methods section. The data is presented as the means ± S.D. of triplicate observations from a single experiment. B – A flow cytometric analysis of the HEK-NK1-R+pEYFP-actin-trasfected cell line at different passage numbers. Histogram plots show the green fluorescence of pEYFP-expressing cells from passage numbers 3, 9 and 15.

Transfected cell line characteristics – pEYFP-actin expression

Next, we examined the passage-dependent effect on the pEYFP-actin expression via FCA and quantitative RT-PCR. Again, cells from the same passage numbers (PN3, PN9 and PN15) were analyzed. FCA revealed an initial decrease in the number of pEYFP-actin-expressing cells (compare the histogram plots between cells from PN3 and PN9; Fig. 2B), while no additional substantial decrease was observed after the six subsequent passages (Fig. 2B). Quantitative RT-PCR analysis was then used to assess the mRNA expression levels of the total β-actin (WT and pEYFP-tagged β-actin) and tagged pEYFP-actin (Tab. 1). The expression level of the total β-actin in the HEK-NK1-R+pEYFP-actin PN3 cells was around 1.9-fold higher than that of endogenous β-actin in the HEK-293 cells, while the levels of total β-actin in the PN9 and PN15 cells and endogenous β-actin in the HEK-293 cells were comparable. pEYFP-actin expression was detected only in the HEK-NK1-R+pEYFP-actin-transfected cell line. The expression level of the total β-actin in cells from PN3, PN9 and PN15 was around 6.5-, 7.2- and 8-fold higher than the corresponding pEYFP-actin expression level (see Tab. 1). This suggests that pEYFP-actin mRNA respectively accounted for approximately 15, 13 and 12.5% of the total β-actin in the PN3, PN9 and PN15 HEK-NK1-R+pEYFP-actin transfected cell lines.

Tab. 1. The relative quantification of the total β-actin and pEYFP-actin via real-time polymerase chain reaction (RT-PCR).

Cell line	ΔCt (total β-actin - 18s)	$2^{-\Delta\Delta Ct}$	ΔCt (pEYFP-actin - 18s)	$2^{-\Delta\Delta Ct}$
HEK-293	11.72 ± 0.03	1	-	-
HEK-NK1-R+pEYFP-actin PN3	10.76 ± 0.17	1.94 ± 0.24	13.47 ± 0.08	6.54 ± 0.35
HEK-NK1-R+pEYFP-actin PN9	11.67 ± 0.07	1.04 ± 0.05	14.51 ± 0.05	7.16 ± 0.25
HEK-NK1-R+pEYFP-actin PN15	11.57 ± 0.13	1.11 ± 0.10	14.57 ± 0.06	8.00 ± 0.33

We used the comparative Ct method (ΔCt) to perform a relative quantification of the target transcripts, with total β-actin representing both endogenous WT and pEYFP-tagged β-actin and pEYFP-actin normalized to the endogenous control 18s rRNA. The $2^{-\Delta\Delta Ct}$ method was used to analyze the relative changes in gene expression between the tested cell lines. 18s rRNA was used as an internal control for each cDNA sample, with the Ct cycle threshold calculated as the cycle at which the fluorescence signal passes a fixed threshold line, ΔCt = Ct(target gene) - Ct(18s), and $2^{-\Delta\Delta Ct}$ representing fold change.

Transfected cell line characteristics – the functional characterization of pEYFP-actin

To further evaluate the effectiveness of the FCS and the suitability of pEYFP-actin as a marker of endogenous actin, we performed confocal microscopy experiments. Consistent with the FCA, the confocal microscopy confirmed that the subpopulation of pEYFP-actin-expressing cells was substantially increased in the HEK-NK1-R+pEYFP-actin transfected cell line (data not shown). Co-localization studies were then conducted in the HEK-NK1-R+pEYFP-actin-transfected cells using rhodamine-phalloidine to stain the actin cytoskeleton. In addition, we evaluated the effects of the NK1-R agonist SP and that of jasplakinolide, an actin-targeting peptide, on the actin cytoskeleton organization (Fig. 3). pEYFP-actin and rhodamine-phalloidine signals were acquired sequentially to prevent the possibility of spectral overlap. In the control (untreated) cells (Fig. 3A), the pEYFP-actin fluorescent signal was mainly restricted to the peripheral region of the cytoplasm, where a fine cortical actin network is located just beneath the cell membrane. A dispersed pEYFP-actin signal was also observed throughout the cytoplasm (Fig. 3A, left panel). Cells stained with rhodamine-phalloidine (Fig. 3A, middle panel), which stains only filamentous actin (F-actin), showed a similar staining pattern, and this co-localization is shown in Fig. 3A, right panel. The co-localization of the pEYFP-actin and F-actin structures (cortical F-actin and short F-actin filaments) is evident. After the activation of the NK1-R with an agonist SP (Fig. 3B, left panel), actin cytoskeleton reorganization was observed. In comparison with the control cells, the cortical signal of the SP-treated cells was stronger: stress fibers and noticeable short F-actin filaments appeared in the cytoplasm. Similar

changes were also observed in the corresponding rhodamine-phalloidine-stained cells (Fig. 3B, middle panel). Again, a high degree of co-localization between pEYFP-actin and the rhodamine-phalloidine F-actin structures (cortical F-actin, short F-actin filaments/aggregates and stress fibers) was observed (Fig. 3B, right panel). There is also a visible increase in the surface area of the SP-treated cells compared to the untreated controls (compare Figs 3A and B). However, there were no major differences between the endogenous F-actin structures and the F-actin structures with incorporated pEYFP-actin with regard to form, cellular distribution and receptor-mediated response. We also tested the effect of jasplakinolide to further functionally characterise the pEYFP-actin (Fig. 3C).

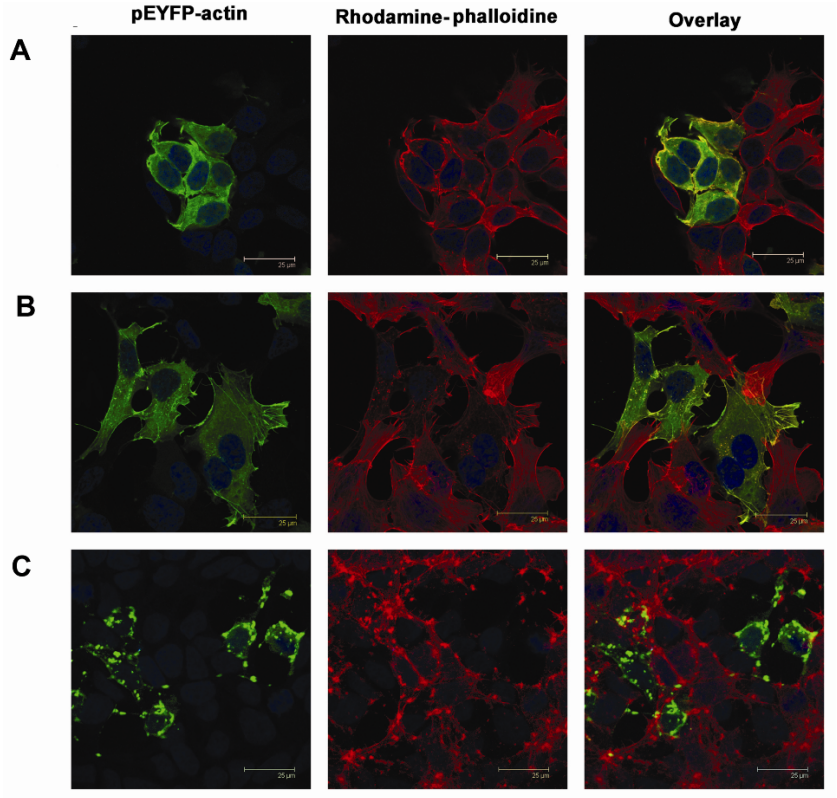

Fig. 3. The co-localization of pEYFP-actin with rhodamine-phalloidine-stained F-actin structures in the HEK-NK1-R+pEYFP-actin-transfected cell line. The pEYFP-actin and rhodamine-phalloidine-stained F-actin structure distribution pattern and colocalization is shown in: A – control (unstimulated) cells; B – cells treated with substance P (1 μM for 10 min at 37ºC); and C – cells treated with jasplakinolide (100 nM for 2 h at 37ºC). The nuclei were counterstained with TO-PRO3 iodide. The green color indicates pEYFP-actin; red is rhodamine-phalloidine-stained F-actin; blue is nuclei; and yellow/orange is the overlapping region indicating colocalization of pEYFP-actin and rhodamine-phalloidine-stained actin structures.

Jasplakinolide was previously shown to disrupt actin filaments and induce polymerization of monomeric actin into amorphous masses in cultured cells [25]. It also competitively inhibits the binding of phalloidin to F-actin [23] and is cell permeable, and therefore suitable to monitor actin-dependent processes in living cells [26]. In HEK-NK1-R+pEYFP-actin-transfected cells, jasplakinolide caused an almost complete disappearance of F-actin structures. Instead, thick actin bundles/aggregates were formed and were located either in the vicinity of the plasma membrane or scattered in the cytoplasm. The pEYFP-actin and rhodamine-phalloidine-stained structures displayed comparable forms and distribution patterns, and a certain degree of co-localization (Fig. 3C).

DISCUSSION

The choice of the cloning technique/selection procedure and methods for monitoring the expression level and biological activity of the expressed transgenes is very important for the generation of a transfected cell line. In this study, we combined the cloning ring technique with FCS to enrich the cell population co-expressing NK1-R and pEYFP-actin. We determined the expression level of the proteins and made a functional characterization of the established transfected cell line by means of RT-PCR, ELISA, receptor radioligand binding and second messenger assays, pharmacological treatments, and confocal microscopy. Our goal was to express NK1-R at a level above the typical 7TM receptor concentration (~10,000/cell) [27] and to keep the expression level of the pEYFP-actin below 30% of the total β-actin, as it was previously found that only actin filaments containing ≤ 30% of GFP-actin retained functional integrity [5]. An initial attempt to establish a stable cell line co-expressing NK1-R and pEYFP-actin using the cloning ring technique was not successful, as it did not yield clones with the anticipated characteristics. In particular, the pEYFP-actin expressing subpopulation of cells in the isolated clones was too small (only up to around 0.1% as revealed by FCA). The efficiency of the cloning ring technique is often low, and it frequently yields a heterogeneous cell population due to the migration of the surrounding cells into the colony during the early growth period [18]. The other possible explanation for the low percentage of pEYFP-actin-expressing cells is gene silencing, which can occur either due to position effect variegation [28] or due to DNA methylation (reviewed in [29]). Similarly, it was reported that it was nearly impossible to obtain a sufficient expression level of another autofluorescently tagged cytoskeleton protein, namely β-tubulin-GFP, in mammalian cells probably due to a post-transcriptional regulation [5]. We therefore utilized FCS to enrich the pEYFP-actin-expressing subpopulation of cells, and then monitored the passage-dependent effect on transgene expression. Although the NK1-R surface expression in the cells from the tested passages (passage numbers 3, 9 and 15) was rather constant, a decrease in the pEYFP-actin expression was observed in particular between cells from passages number 3 and 9, while it remained relatively constant between the cells from passages

number 9 and 15. It was previously demonstrated that the steady-state level of actin autoregulates net actin synthesis to maintain an optimal homeostatic cellular concentration of actin [30]. Our quantitative RT-PCR data suggested that cells from passages number 9 and 15, but not cells from passage number 3, have comparable total β-actin mRNA levels to those of untrasfected HEK-293 cells. It is therefore plausible to suggest that the autoregulatory feedback of actin concentration could be responsible for the initial decrease in pEYFP-actin expression. We also complied with the suggested recommendations for minimizing/avoiding passage-dependent effects such as the use of high-quality starting material from a known biological source, and a standardized cell environment and cell culture technique [16]. It was previously found that GFP-actin was fully functional in *in vitro* motility experiments when the fusion protein did not exceed 30% of the native actin content [31]. In order to control this requirement, quantitative RT-PCR analysis was used to assess the mRNA expression level of total β-actin and pEYFP-actin. The results showed that the pEYFP-actin level in the cells from the passages tested was within the required limits. We are aware that mRNA and protein expression ratios do not correlate directly; however, this method enabled fast and efficient tracking of transfection stability and estimation of the pEYFP-actin:endogenous β-actin ratio in cells after a defined number of passages. The malfunctioning of pEYFP-actin could also result from the steric hindrance and position of the GFP-tag [32] as well as the altered proportion of actin isoforms on account of overexpressed β-actin [33]. In the utilized construct, the pEYFP tag was fused to the N-terminus of the β-actin, as it was previously demonstrated that only the N-terminally positioned GFP-tag yielded the correct folding and preserved functionality of the actin fusion partner [32, 34]. Further evidence that the pEYFP-actin fusion protein did not disturb actin function was shown by co-localization experiments and pharmacological treatments. Co-localization between pEYFP-actin and rhodamine-phalloidine-stained F-actin structures implied the successful incorporation of the fluorescent fusion protein into the actin filaments. Previous studies also reported an overlay mainly between the EYFP-tagged actin and rhodamine-phalloidine-stained cortical F-actin and stress fibers [17, 33]. Changes observed in the NK1-R agonist- and jasplakinolide-treated cells further indicate that actin polymerization and F-actin structure formation is not disturbed by pEYFP-actin. The $G\alpha_{q/11}$-coupled NK1-R-mediated effect on the cytoskeleton organization is in agreement with previous reports demonstrating $G\alpha_{q/11}$-dependent rearrangement of the actin cytoskeleton (reviewed in [2]). Comparable results were also obtained with another $G\alpha_{q/11}$-coupled 7TM receptor, namely thyrotropin-releasing hormone type 1 receptor [35]. Additional evidence for the functionality of the pEYFP-actin in the generated transfected cell line was provided by jasplakinolide treatment. *In vitro,* jasplakinolide accelerates actin polymerization, lowers the critical concentration of actin assembly and stabilizes the F-actin structures [23, 36], while in cultured cells, it disrupt actin filaments and induces polymerization of monomeric actin into

amorphous masses [25]. The pEYFP-actin and rhodamine-phalloidine-stained F-actin aggregate formation were also observed in the transfected cell line (HEK-NK1-R+pEYFP-actin) when it was exposed to jasplakinolide.
In conclusion, this study reports on the generation and rigorous functional characterization of a transfected cell line co-expressing NK1-R and pEYFP-actin. pEYFP-actin was proved to be suitable marker of endogenous actin, and in this regard, the generated transfected cell line provides a valuable tool for the study of 7TM receptor-mediated reorganization of the actin cytoskeleton in living cells.

Acknowledgments. The authors would like to thank Magdalena Dobravec for her excellent technical assistance. This study was supported by the Slovenian Research Agency (program P4-0053).

REFERENCES

1. Janmey, P.A. The cytoskeleton and cell signaling: component localization and mechanical coupling. **Physiol. Rev.** 78 (1998) 763-781.
2. Luttrell, L.M. Big G, little G: G proteins and actin cytoskeletal reorganization. **Mol. Cell.** 9 (2002) 1152-1154.
3. Cotton, M. and Claing, A. G protein-coupled receptors stimulation and the control of cell migration. **Cell. Signal.** 21 (2009) 1045-1053.
4. Ludin, B., Doll, T., Meili, R., Kaech, S. and Matus, A. Application of novel vectors for GFP-tagging of proteins to study microtubule-associated proteins. **Gene** 173 (1996) 107-111.
5. Ludin, B. and Matus, A. GFP illuminates the cytoskeleton. **Trends Cell. Biol.** 8 (1998) 72-77.
6. Lippincott-Schwartz, J. and Patterson, G.H. Development and use of fluorescent protein markers in living cells. **Science** 300 (2003) 87-91.
7. Yoon, Y., Pitts, K. and McNiven, M. Studying cytoskeletal dynamics in living cells using green fluorescent protein. **Mol. Biotechnol.** 21 (2002) 241-250.
8. Bohme, I. and Beck-Sickinger, A.G. Illuminating the life of GPCRs. **Cell. Commun. Signal.** 7 (2009) - *in press* (doi:10.1186/1478-811X-7-16).
9. Arun, K.H., Kaul, C.L. and Ramarao, P. Green fluorescent proteins in receptor research: an emerging tool for drug discovery. **J. Pharmacol. Toxicol. Methods** 51 (2005) 1-23.
10. Volovyk, Z.M., Wolf, M.J., Prasad, S.V. and Rockman, H.A. Agonist-stimulated β-adrenergic receptor internalization requires dynamic cytoskeletal actin turnover. **J. Biol. Chem.** 281 (2006) 9773-9780.
11. Ganguly, S., Pucadyil, T.J. and Chattopadhyay, A. Actin cytoskeleton-dependent dynamics of the human serotonin1A receptor correlates with receptor signaling. **Biophys. J.** 95 (2008) 451-463.

12. Barnes, W.G., Reiter, E., Violin, J.D., Ren, X.R., Milligan, G. and Lefkowitz, R.J. β-Arrestin 1 and $G\alpha_{q/11}$ coordinately activate RhoA and stress fiber formation following receptor stimulation. **J. Biol. Chem.** 280 (2005) 8041-8050.
13. Vogt, S., Grosse, R., Schultz, G. and Offermanns, S. Receptor-dependent RhoA activation in G_{12}/G_{13}-deficient cells: genetic evidence for an involvement of G_q/G_{11}. **J. Biol. Chem.** 278 (2003) 28743-28749.
14. Le Page, S.L., Bi, Y. and Williams, J.A. CCK-A receptor activates RhoA through $G\alpha_{12/13}$ in NIH3T3 cells. **Am. J. Physiol. Cell. Physiol.** 285 (2003) 1197-1206.
15. Gohla, A., Offermanns, S., Wilkie, T.M. andSchultz, G. Differential involvement of $G\alpha_{12}$ and $G\alpha_{13}$ in receptor-mediated stress fiber formation. **J. Biol. Chem.** 274 (1999) 17901-17907.
16. Pagliaro, L. and Praestegaard, M. Transfected cell lines as tools for high throughput screening: a call for standards. **J. Biomol. Screen.** 6 (2001) 133-136.
17. Herget-Rosenthal, S., Hosford, M., Kribben, A., Atkinson, S.J., Sandoval, R.M. and Molitoris, B.A. Characteristics of EYFP-actin and visualization of actin dynamics during ATP depletion and repletion. **Am J. Physiol. Cell. Physiol.** 281 (2001) 1858-1870.
18. McFarland, D.C. Preparation of pure cell cultures by cloning. **Methods Cell. Sci.** 22 (2000) 63-66.
19. Martini, L., Hastrup, H., Holst, B., Fraile-Ramos, A., Marsh, M. and Schwartz, T.W. NK1 receptor fused to β-arrestin displays a single-component, high-affinity molecular phenotype. **Mol. Pharmacol.** 62 (2002) 30-37.
20. Kubale, V., Abramovič, Z., Pogačnik, A., Heding, A., Šentjurc, M. and Vrecl, M. Evidence for a role of caveolin-1 in neurokinin-1 receptor plasma-membrane localization, efficient signaling, and interaction with β-arrestin 2. **Cell. Tissue Res.** 330 (2007) 231-245.
21. Ramsay, D., Kellett, E., McVey, M., Rees, S. and Milligan, G. Homo- and hetero-oligomeric interactions between G-protein-coupled receptors in living cells monitored by two variants of bioluminescence resonance energy transfer (BRET): hetero-oligomers between receptor subtypes form more efficiently than between less closely related sequences. **Biochem. J.** 365 (2002) 429-440.
22. Vrecl, M., Anderson, L., Hanyaloglu, A., McGregor, A.M., Groarke, A.D., Milligan, G., Taylor, P.L. and Eidne, K.A. Agonist-induced endocytosis and recycling of the gonadotropin-releasing hormone receptor: effect of β -arrestin on internalization kinetics. **Mol. Endocrinol.** 12 (1998) 1818-1829.
23. Bubb, M.R., Senderowicz, A.M., Sausville, E.A., Duncan, K.L. and Korn, E.D. Jasplakinolide, a cytotoxic natural product, induces actin polymerization and competitively inhibits the binding of phalloidin to F-actin. **J. Biol. Chem.** 269 (1994) 14869-14871.

24. Holst, B., Zoffmann, S., Elling, C.E., Hjorth, S.A. and Schwartz, T.W. Steric hindrance mutagenesis versus alanine scan in mapping of ligand binding sites in the tachykinin NK1 receptor. **Mol. Pharmacol.** 53 (1998) 166-175.
25. Bubb, M.R., Spector, I., Beyer, B.B. and Fosen, K.M. Effects of jasplakinolide on the kinetics of actin polymerization. An explanation for certain *in vivo* observations. **J. Biol. Chem.** 275 (2000) 5163-5170.
26. Cramer, L.P. Role of actin-filament disassembly in lamellipodium protrusion in motile cells revealed using the drug jasplakinolide. **Curr. Biol.** 9 (1999) 1095-1105.
27. Ostrom, R. S. and Insel, P.A. The evolving role of lipid rafts and caveolae in G protein-coupled receptor signaling: implications for molecular pharmacology. **Br. J. Pharmacol.** 143 (2004) 235-245.
28. Birchler, J.A., Bhadra, M.P. and Bhadra, U. Making noise about silence: repression of repeated genes in animals. **Curr. Opin. Genet. Dev.** 10 (2000) 211-216.
29. Hsieh, C.L. Dynamics of DNA methylation pattern. **Curr. Opin. Genet. Dev.** 10 (2000) 224-228.
30. Leavitt, J., Ng, S.Y., Varma, M., Latter, G., Burbeck, S., Gunning, P. and Kedes, L. Expression of transfected mutant β-actin genes: transitions toward the stable tumorigenic state. **Mol. Cell. Biol.** 7 (1987) 2467-2476.
31. Doyle, T. and Botstein, D. Movement of yeast cortical actin cytoskeleton visualized *in vivo*. **Proc. Natl. Acad. Sci. USA.** 93 (1996) 3886-3891.
32. Westphal, M., Jungbluth, A., Heidecker, M., Muhlbauer, B., Heizer, C., Schwartz, J.M., Marriott, G. and Gerisch, G.. Microfilament dynamics during cell movement and chemotaxis monitored using a GFP-actin fusion protein. **Curr. Biol.** 7 (1997) 176-183.
33. Ballestrem, C., Wehrle-Haller, B. and Imhof, B. A. Actin dynamics in living mammalian cells. **J. Cell. Sci.** 111 (1998) 1649-1658.
34. Verkhusha, V.V., Shavlovsky, M.M., Nevzglyadova, O.V., Gaivoronsky, A.A., Artemov, A.V., Stepanenko, O.V., Kuznetsova, I.M. and Turoverov, K.K. Expression of recombinant GFP-actin fusion protein in the methylotrophic yeast Pichia pastoris. **FEMS Yeast Res.** 3 (2003) 105-111.
35. Hrovat, A., Frangež, R., Pogačnik, A. and Vrecl, M. Actin cytoskeleton rearrangement in cells after the activation of membrane-bound receptor for thyrotropin-releasing hormone. **Slov. Vet. Res.** 40 (2003) 181-189.
36. Visegrady, B., Lorinczy, D., Hild, G., Somogyi, B. and Nyitrai, M. The effect of phalloidin and jasplakinolide on the flexibility and thermal stability of actin filaments. **FEBS Lett.** 565 (2004) 163-166.